Acta Crystallographica Section D
Biological Crystallography
ISSN 0907-4449

Structure of circularly permuted $DsbA_{Q100T99}$: preserved global fold and local structural adjustments

Babu A. Manjasetty,[a]‡ Jens Hennecke,[b]§ Rudi Glockshuber[b] and Udo Heinemann[a,c]*

[a]Forschungsgruppe Kristallographie, Max-Delbrück-Centrum für Molekulare Medizin, D-13092 Berlin, Germany, [b]Institute of Molecular Biology and Biophysics, Eidgenössische Technische Hochschule, Hönggerberg, CH-8093 Zürich, Switzerland, and [c]Institut für Chemie – Kristallographie, Freie Universität Berlin, Takustrasse 6, D-14195 Berlin, Germany

‡ On leave from the Department of Physics, Government Science College, Bangalore 560 002, India.
§ Present address: Micromet AG, Am Klopferspitz 19, D-82152 Martinsried/Planegg, Germany.

Correspondence e-mail: heinemann@mdc-berlin.de

Received 3 September 2003
Accepted 12 December 2003

PDB Reference:
$DsbA_{Q100T99}$, 1un2, r1un2sf.

The thiol-disulfide oxidoreductase DsbA is required for efficient formation of disulfide bonds in the *Escherichia coli* periplasm. The enzyme is the strongest oxidant of the family of thioredoxin-like proteins and three-dimensional structures of both oxidized and reduced forms are known. DsbA consists of a catalytic thioredoxin-like domain and a helical domain that is inserted into the thioredoxin motif. Here, the X-ray structure of a circularly permuted variant, $cpDsbA_{Q100T99}$, is reported in which the natural termini are joined by the pentapeptide linker GGGTG, leading to a continuous thioredoxin domain, and new termini that have been introduced in the helical domain by breaking the peptide bond Thr99–Gln100. $cpDsbA_{Q100T99}$ is catalytically active *in vivo* and *in vitro*. The crystal structure of oxidized $cpDsbA_{Q100T99}$, determined by molecular replacement at 2.4 Å resolution, was found to be very similar to that of wild-type DsbA. The lower thermodynamic stability of $cpDsbA_{Q100T99}$ relative to DsbA is associated with small structural changes within the molecule, especially near the new termini and the circularizing linker. The active-site helices and adjacent loops display increased flexibility compared with oxidized DsbA.

1. Introduction

Formally, any open chain can undergo a circular permutation of its structure through the covalent connection of its natural termini and the generation of new termini at a different position in the chain (Heinemann & Hahn, 1995*a*). Several examples of proteins that have undergone a circular permutation during molecular evolution have been described (Heinemann & Hahn, 1995*b*; Lindqvist & Schneider, 1997; Murzin, 1998*a*,*b*; Jung & Lee, 2001; Uliel *et al.*, 2001). The two main strategies to achieve a circular permutation in a protein artificially are (i) peptide-bond cleavage *in vitro* and covalent coupling of the native polypeptide-chain termini (Goldenberg & Creighton, 1983) and (ii) the rearrangement of coding genes by rational or random genetic engineering (Luger *et al.*, 1989; Graf & Schachman, 1996; Hennecke *et al.*, 1999; Rojas *et al.*, 1999). Permutation experiments have mainly been performed with proteins in which the natural N- and C-termini are in close proximity, as is often observed (Thornton & Sibanda, 1983).

In experiments designed to identify segments (nuclei) in a polypeptide chain that are required for folding and stability, circularly permuted proteins were shown to retain folding competence generally, but permutations often resulted in protein variants that were less stable than the corresponding wild type (Goldenberg & Creighton, 1983; Luger *et al.*, 1989; Hennecke *et al.*, 1999; Iwakura *et al.*, 2000; Li & Shakhnovich,

2001; Barrientos *et al.*, 2003; Cheltsov *et al.*, 2003). Although many circularly permuted variants have been studied biochemically, only a few crystallographic or NMR studies of circularly permuted proteins have been described (Hahn *et al.*, 1994; Viguera *et al.*, 1996; Pieper *et al.*, 1997; Aÿ *et al.*, 1998; Chu *et al.*, 1998; Wright *et al.*, 1998; Tougard *et al.*, 2002; Barrientos *et al.*, 2003).

DsbA is a monomeric 189-residue protein that catalyzes the introduction of disulfide bonds into newly secreted polypeptides in the *Escherichia coli* periplasm (Bardwell *et al.*, 1991; Ritz & Beckwith, 2001; Collet & Bardwell, 2002). The enzyme has a very reactive catalytic disulfide bond with the sequence Cys30-Pro31-His32-Cys33 and randomly introduces disulfides into secretory proteins (Zapun *et al.*, 1993, 1994; Nelson & Creighton, 1994; Wunderlich *et al.*, 1995). DsbA is the strongest oxidant within the family of thioredoxin-like oxidoreductases (E'_o = −120 to −125 mV; Wunderlich *et al.*, 1993; Zapun *et al.*, 1993; Hennecke *et al.*, 1999), which mainly results from the extremely low pK_a of 3.4 of the nucleophilic active-site residue Cys30 (Nelson & Creighton, 1994). The three-dimensional structures of the oxidized and reduced form of DsbA have been determined by NMR spectroscopy and X-ray crystallography (Martin *et al.*, 1993; Guddat, Bardwell, Zander *et al.*, 1997; Guddat *et al.*, 1998; Schirra *et al.*, 1998), revealing that the structure of reduced DsbA is very similar to that of the oxidized form. In reduced DsbA, the thiolate anion is mainly stabilized by the partial positive charge from the dipole of the active-site helix (Cys30 is the most N-terminal residue of α-helix 1). His32 appears to contribute about one pK_a unit to the lowered pK_a of Cys30 (Kortemme *et al.*, 1996) and three hydrogen bonds from the thiol of Cys33 and the amine H atoms of His32 and Cys33 further stabilize the Cys30 thiolate (Guddat *et al.*, 1998).

The circularly permuted variant cpDsbA$_{Q100T99}$ analyzed in this study resulted from a recent random circular permutation experiment on DsbA in which the natural termini were linked by the pentapeptide linker GGGTG and biologically active permuted variants with new termini were selected *in vivo* (Hennecke *et al.*, 1999). This study revealed that the helices α2, α3, α5 and α6, all of which are located in the helical domain, may not be disrupted without loss of folding competence and are obviously essential for folding and stability. cpDsbA$_{Q100T99}$ has its new N-terminus in the helical domain at residue Gln100 in the loop between helices α3 and α4. The permuted variant is catalytically active both *in vivo* and *in vitro* and almost as oxidizing as the wild type (E'_o = −130 mV; Hennecke *et al.*, 1999). We have crystallized the oxidized form of cpDsbA$_{Q100T99}$, which is 5 kJ mol^{-1} less stable than oxidized DsbA and shows cooperative two-state denaturant-induced unfolding (Hennecke *et al.*, 1999). Here, we describe the X-ray structure of cpDsbA$_{Q100T99}$ and compare it with the structure of wild-type DsbA.

2. Experimental

The circularly permuted DsbA variant cpDsbA$_{Q100T99}$ was isolated from recombinant *E. coli* cells, purified as described previously (Hennecke *et al.*, 1999) and crystallized at 291 K employing the hanging-drop vapour-diffusion technique. The drop consisted of 1.5 µl of 15 mg ml^{-1} protein dissolved in water mixed with 1.5 µl of reservoir solution (25% PEG 8000, 7–10% DMSO, 0.1 *M* cacodylate pH 6.5). Crystals belong to space group $P2_1$, with unit-cell parameters a = 37.8, b = 52.6, c = 53.7 Å, β = 103.4° and one molecule in the asymmetric unit (45% solvent content). X-ray diffraction data were collected at beamline X11 at the EMBL Outstation at DESY (Hamburg, Germany) under cryocooling. Measured data were integrated, scaled and merged using the programs *DENZO* and *SCALEPACK* (Otwinowski & Minor, 1997). Crystallographic data are presented in Table 1.

Table 1
Data-collection and refinement statistics.

Statistics for the highest resolution shell (2.46–2.4 Å) are given in parentheses.

Data collection	
Wavelength (Å)	0.91160
Resolution (Å)	2.4
Total observations	37723
Unique observations	7952
Completeness (%)	99.0 (98.1)
R_{sym}	0.056 (0.099)
Average $I/\sigma(I)$	17.4 (6.4)
Refinement	
Resolution range (Å)	20–2.4
No. reflections	7149
No. reflections in R_{free} set	791
R factor†	0.206
Free R factor‡	0.256
R.m.s.d. bond lengths (Å)	0.009
R.m.s.d. bond angles (°)	1.027
No. non-H atoms	1447
Average B factor (Å^2)	42.7

† $R = \sum_h \sum_i \big||F_o(h)| - k|F_c(h)|\big| / \sum_h |F_o(h)|$. ‡ The free R factor was calculated using a 5% randomly selected subset of the total number of reflections.

The structure of cpDsbA$_{Q100T99}$ was solved by molecular replacement using the program *AMoRe* (Navaza, 2001). The crystal structure of DsbA (OX2; PDB code 1a2j) was used as the starting model. For the initial resolution range 7.0–3.5 Å, the rotation search gave a clear solution for the single molecule in the asymmetric unit at 14.4σ, with the second peak at 4.6σ. The translation search using the top peak and a resolution range 20.0–4.5 Å in space group $P2_1$ gave a maximum with a correlation coefficient of 0.624 and an R value of 38.8%. Density improvement and removal of model bias was achieved by the free-atom refinement method in *ARP*/*wARP* (Perrakis *et al.*, 2001). Model building was performed using *O* (Jones *et al.*, 1991) and the model was refined using the program *REFMAC* (Murshudov *et al.*, 1997; Potterton *et al.*, 2003) with TLS parameters (Winn *et al.*, 2001) (see Table 1 for statistics). The final model includes 186 of the 197 residues of cpDsbA$_{Q100T99}$ and 82 water molecules. The two residues Ile99b and Lys99c at the new C-terminus were not modelled owing to poorly defined electron density. Residues Ala1 and Gln2 at the natural amino-terminus, Lys188 and Lys189 at the natural C-terminus, and Gly190, Gly191, Gly192, Thr193 and Gly194 of the linker pentapeptide had weak electron density and were also not included in refinement. The coordinates and

structure factors have been deposited with the Protein Data Bank with the accession code 1un2. All molecular drawings were produced with *MOLSCRIPT* (Kraulis, 1991), *BOBSCRIPT* (Esnouf, 1999) and *Raster3D* (Merritt & Murphy, 1994).

3. Results and discussion

3.1. Overall structure after circular permutation

The main features of the three-dimensional structure of wild-type DsbA (Martin *et al.*, 1993; Guddat, Bardwell, Zander *et al.*, 1997) are retained in the structure of cpDsbA$_{Q100T99}$ (Fig. 1). A continuous thioredoxin-like domain is formed by residues Ala1–Asn62, Glu139–Lys189 and the pentapeptide connecting the natural termini (Gly190–Gly194). The domain consists of a five-stranded β-sheet ($\beta1$–$\beta5$) covered on one side by helices ($\alpha1$ and $\alpha7$) that are roughly parallel to the strands and on the other side by a helix ($\alpha6$) oriented almost perpendicular to the direction of the strands. The compactly folded helical domain formed by residues Phe63–Gln138 consists of an antiparallel three-helix bundle ($\alpha2$, $\alpha3$ and $\alpha4$) with two additional helices ($\alpha5$ and half of $\alpha6$) that wrap around the bundle. This domain now carries the polypeptide-chain termini, which are inserted between $\alpha3$ and $\alpha4$ into the three-helix bundle, which represents an unusual fold. The long helix $\alpha6$ links the two domains. Three additional residues, Leu99a, Ile99b and Lys99c, at the C-terminus result from the genetic construction of the library of randomly circularly permuted *dsbA* genes from which the cpDsbA$_{Q100T99}$ variant was selected (Hennecke *et al.*, 1999).

The variant cpDsbA$_{Q100T99}$ adopts a three-dimensional structure very similar to that of the oxidized wild-type protein, proving that the circular permutation of its sequence and the shift of the chain termini from one protein domain into the other does not prevent native-like folding. This observation is significant in view of the fact that the circularly permuted variant differs from DsbA in one important aspect: in the latter, the sequentially continuous non-catalytic helical domain is inserted into the catalytic thioredoxin-like domain which carries the chain termini. In cpDsbA$_{Q100T99}$, a sequentially continuous thioredoxin-like domain is inserted into the helical domain where the polypeptide chain begins and ends. Obviously, this fundamentally reorganized protein topology is still compatible with native-like folding, physical properties and enzymatic function. It is envisaged that the majority of the DsbA variants generated by random circular permutation (Hennecke *et al.*, 1999) have likewise retained their native-like form, although detailed structural data are not available for these proteins. Similarly, a phosphoglycerate kinase variant has recently been reported to have retained native-like structure after a circular permutation that moved the chain termini from one globular domain of the protein into the other (Tougard *et al.*, 2002).

3.2. Structural changes

Three different crystal structures of oxidized wild-type DsbA have been reported to which cpDsbA$_{Q100T99}$ may be compared. Crystal form 1 of oxidized DsbA (OX1; Martin *et al.*, 1993; Guddat, Bardwell, Zander *et al.*, 1997) was refined at 1.7 Å resolution in space group *C*2 with two monomers in the asymmetric unit. Form 2 (OX2; Guddat *et al.*, 1998) was refined at 2.0 Å resolution in $P2_1$ with one monomer in the asymmetric unit and form 3 (OXR; Guddat *et al.*, 1998) was determined at 2.7 Å resolution in $P2_12_12$ with two monomers in the asymmetric unit. The overall structure of cpDsbA$_{Q100T99}$ is similar to that of DsbA: the r.m.s. deviation between 161 C^{α} positions of cpDsbA$_{Q100T99}$ and the corresponding atoms of OX1A, OX1B, OX2, OXRA and OXRB are 1.03, 0.83, 0.45, 0.69 and 1.0 Å, respectively, after least-squares fitting. These values indicate an overall retention of the global fold. However, there are several local structural changes related to two important differences. The cpDsbA$_{Q100T99}$ crystals were obtained under similar precipitant and pH conditions as the OX1 crystal (25% PEG 8000, 10% MPD, 0.1 *M* cacodylate pH 6.5), but the unit-cell parameters are comparable with those of OX2 (a = 38.5, b = 51.4, c = 42.5 Å, β = 103.8° and one

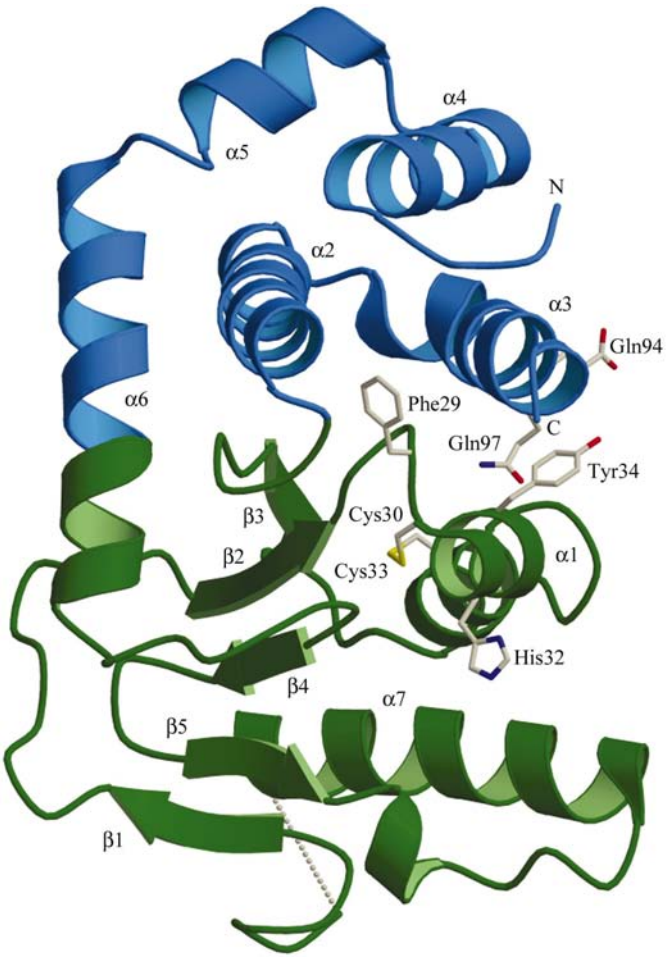

Figure 1
Crystal structure of oxidized cpDsbA$_{Q100T99}$ from *E. coli*. The helical domain of cpDsbA$_{Q100T99}$ is coloured blue and the thioredoxin-like domain green. The side chains of functionally important residues discussed in the text are shown. The new amino- and carboxy-termini are labelled. The region of poorly defined electron density for the peptide connecting the N- and C-termini of DsbA is marked by a dotted line.

molecule in the asymmetric unit), with the *c* axis showing the largest change in unit-cell dimension (about 11 Å increase).

In particular, the segments around the new termini adopt new backbone conformations (Fig. 2*a*). Significant changes in φ/ψ values for the new C- and N-terminal residues Gln97, Lys98, Thr99, Gln100, Thr101 and Ile102 are observed. The C^{α} atoms of Gln100 and Thr99 are displaced by 7.4 and 5.3 Å, respectively, from their positions in DsbA (OX2). The side chain of the new amino-terminal residue, Gln100, is rotated by approximately 180° and stabilized by interactions with the side chain of Asn114 of helix α4. At the new C-terminus extending helix α3, two residues beyond Leu99a have poor electron density, probably owing to disorder. The polar residue Gln97 is located near the new carboxy-terminus. This residue has previously been predicted to dictate the difference in redox potential between DsbA and thioredoxin (Gane *et al.*, 1995; Warwicker, 1998). Interestingly, Gln97 adopts a new side-chain conformation, clearly changing the interface between the active site and the helical domain (Fig. 2*b*).

On the other hand, the region around the natural termini in $cpDsbA_{Q100T99}$ retained high intrinsic structural flexibility as in wild-type DsbA structures. No electron density was observed for the C-terminal Lys189 in all DsbA wild-type structures, indicating an inherent flexibility of the C-terminal residue. Because of their different crystal environments, the two independent wild-type monomers of OX1 differ maximally from each other at the N-terminus. Residue Gln2 adopts different conformations in OX1A and OX1B and a very large shift of about 9 Å from the mean coordinate position of Ala1 indicates that the N-terminus is also flexible in the natural protein. In support of these arguments, residue Tyr3 is slightly moved towards the direction of the natural C-terminus with an elevated displacement of 1.0 Å in $cpDsbA_{Q100T99}$. Overall, the electron density is poorly defined for residues Ala1, Gln2 and Lys188 in $cpDsbA_{Q100T99}$. The electron density is also discontinuous and poorly defined for the linker-peptide segment Gly190–Gly194. No electron density is observed for residue Lys189 (the natural C-terminus). Modelling and refinement of these ill-defined residues leads to very high temperature factors of about 100 $Å^2$. Hence, these residues were not included in the final model. Furthermore, analysis of the crystal packing reveals a possible explanation of the observed structural flexibility. The *c* axis shows the largest change in unit-cell parameter (about 11 Å increase) when compared with the OX2 crystals. The molecules are arranged in layers parallel to the *ab* plane. The molecules are significantly shifted along the *c* axis, leading to the formation of large solvent channels. A possible sliding motion of neighbouring layers parallel to the *ab* plane may be the origin of the high thermal motion within the lattice, whereas movement along the *a* and *b* axes is much more restricted owing to the presence of intermolecular contacts. Interestingly, the region around the natural termini (despite the linker) lacks significant contacts with the rest of the protein. However, in other circularly permuted proteins the linker region is clearly defined (Hahn *et al.*, 1994; Aÿ *et al.*, 1998).

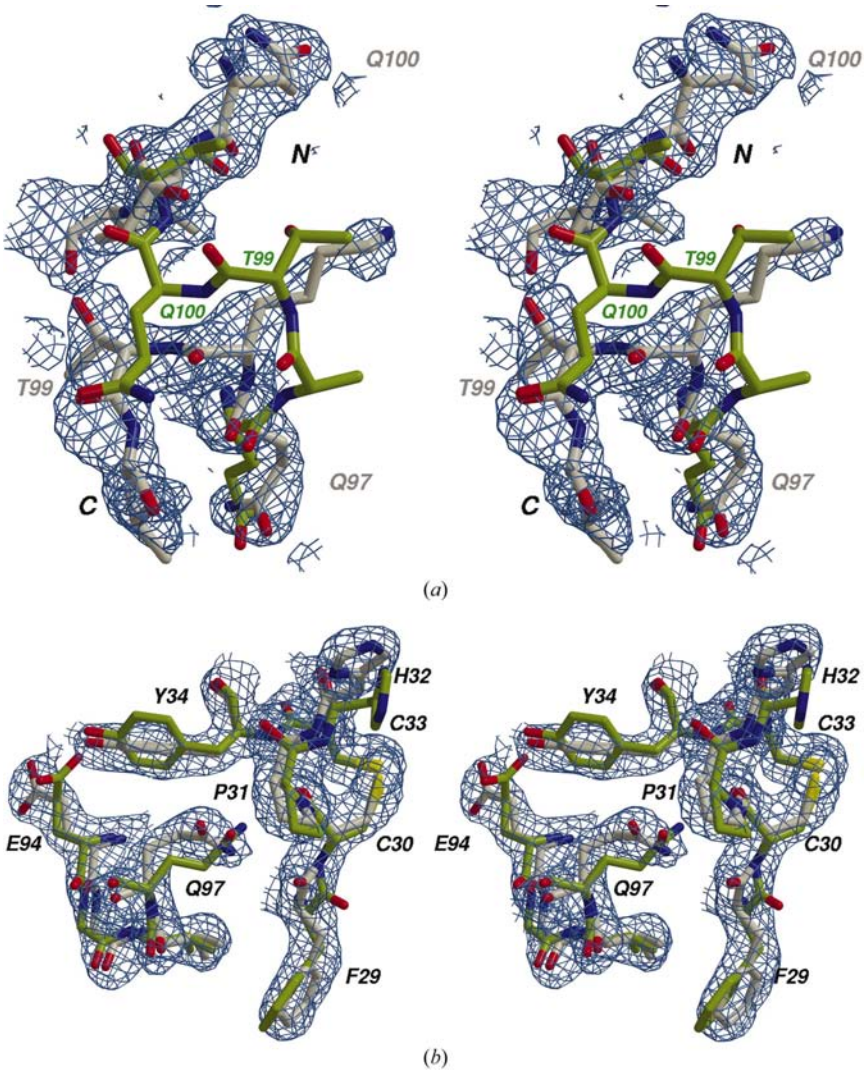

Figure 2
(*a*) The region around the novel termini: the position Q100T99 where the circular permutation was applied to DsbA (OX2, green) after least-squares superposition on the structure of $cpDsbA_{Q100T99}$ (grey). The σ_A-weighted $2F_o - F_c$ electron-density map is contoured at 1.0σ. The new amino- and carboxy-termini are labelled, along with the residues Gln100 and Thr99. The functionally important residue Gln97 in this region is also shown and labelled. (*b*) Conformational change at the active site. The electron density for the active site in $cpDsbA_{Q100T99}$ is well defined and a right-handed conformation of the disulfide is conserved. The side chains of residues His32, Phe29, Tyr34, Gln97 and Glu94 adopt new conformations compared with DsbA (OX2). The colour representation is similar to that in (*a*). The σ_A-weighted $2F_o - F_c$ electron-density map is contoured at 1.0σ.

The overall architecture around the active-site disulfide bond (segment Cys30-Pro31-His32-Cys33) of oxidized cpDsbA$_{Q100T99}$ is similar to that of DsbA and no significant deviation of the peptide backbone is observed for the active-site residues. However, certain details of the environment of the active site differ. Specifically, the side chains of residues Phe29, His32, Tyr34, Glu94 and Gln97 adopt a new conformation in the permuted protein. The structural changes within the active site and its neighbouring residues and the altered mode of interaction with the residues Gln97 and Glu94 from the helical domain are depicted with the electron density in Fig. 2(*b*). The perturbation starts from residue Phe29 and the interactions between Gln97, Phe29, Cys30 and Pro31 are changed. The interatomic contacts Gln97 N$^{\varepsilon2}$—Cys30 O and Gln97 O$^{\varepsilon1}$—Pro31 N of all three forms of wild-type structures are substituted in the structure of cpDsbA$_{Q100T99}$ by Gln97 N$^{\varepsilon2}$—Phe29 O (3.3 Å) and Gln97 N$^{\varepsilon2}$—Cys30 O (4.0 Å). A change in the backbone conformations of residues Phe29 and Cys30 results from the shuffling of polar interactions. The interactions between Glu94 O$^{\varepsilon2}$ and Tyr34 O$^{\eta}$ (2.9 Å in OX2, 4.1 Å in OX1A) and Glu94 O$^{\varepsilon1}$ and Tyr34 O$^{\eta}$ (3.4 Å in OX2, 5.2 Å in OX1A) are comparatively relaxed in cpDsbA$_{Q100T99}$, where corresponding distances of 4.5 and 5.8 Å are observed. The bulky Tyr34 side chain is rotated and adopts a different conformation to that found in the wild-type structures. The other major structural differences concern the side chain of His32. His32, one of the two residues between the active-site cysteines, is critical to the oxidizing power of DsbA and to the relative instability of the protein in the oxidized form. Mutation of this single residue to tyrosine, serine or leucine results in a significant increase in stability (of approximately 20–28 kJ mol^{-1}) of the oxidized His32 variants relative to the oxidized wild-type protein (Guddat, Bardwell, Glockshuber *et al.*, 1997). In cpDsbA$_{Q100T99}$, the side chain of His32 has adopted a new conformation under the influence of the symmetry-related residue Phe129. Although the rearrangement in the active site and the neighbouring residues is significant, it does not affect the right-handed conformation of the disulfide bridge.

Furthermore, the network of ionic interactions observed for DsbA between residue Glu24 from β2, Glu37 from the active-site helix α1 and Glu58 from β3 is rearranged in cpDsbA$_{Q100T99}$ (not shown). This network is thought to influence the physicochemical properties of DsbA (Hu *et al.*, 1997; Jacobi *et al.*, 1997). The biological activity of DsbA has been proposed to be associated with an unusual acidic surface patch formed by Glu24, Glu37, Glu38 and Asp44 from helix α1 of the thioredoxin-like domain, and Glu85, Glu86 and Glu94 from helix α3 of the helical domain (Guddat, Bardwell, Zander *et al.*, 1997). Moreover, in contrast to thioredoxin, the active-site helix of DsbA has a characteristic kink caused by the insertion of the tripeptide Glu38-Val39-Leu40 that separates the active-site helix into two segments. However, previous mutagenesis studies revealed that the kink in the active-site helix alone is not responsible for the unusual redox properties of DsbA (Hennecke *et al.*, 1997). In the permuted variant cpDsbA$_{Q100T99}$, significant conformational changes are observed at the kink and the preceding residue Glu37 compared with wild-type structures. All residues of the acidic patch on the surface of DsbA show changes in side-chain conformation, except for the buried residue Glu24.

The proposed peptide-binding groove of DsbA consists of uncharged polar and hydrophobic residues. In cpDsbA$_{Q100T99}$, it is lined by the residues Phe36 and Leu40 from the helix α1, the active-site *cis*-Pro151, the residue Gln160 from strand β5 and residues Pro163, Gln164, Thr168, Met171, Phe174 and Val175 from the flexible loop region between β5 and the first turn of α7 (Guddat, Bardwell, Zander *et al.*, 1997). The structural changes observed at the peptide-binding groove in cpDsbA$_{Q100T99}$ mainly arise from changes in crystal contacts. Although the symmetry-related contact of Phe129 and its preceding residues at the proposed peptide-binding groove is well conserved, the position of Phe129 is shifted by about 0.5 Å from that observed in OX2. In the structures of wild-type DsbA, it was presumed that the widening of the groove depends upon crystal contacts with symmetry-related molecules (Guddat *et al.*, 1998). High flexibility, as shown by elevated structural deviations, is restricted to the loop between β5 and α7 in cpDsbA$_{Q100T99}$. Similar observations can be made in the wild-type structures. In contrast to these arguments, the flexibility of the supposed substrate-binding region in cpDsbA$_{Q100T99}$ is restricted to the active-site helices. The loop between β5 and α7 is stabilized by intermolecular and intramolecular interactions

3.3. Functional implications of the circular permutation

Several residues, including His32 between the active-site cysteines, the polar Gln97 from the helical domain, the acidic Glu37 and the kink in the active-site helix, have been proposed to influence the redox potential of the protein (Gane *et al.*, 1995; Kortemme *et al.*, 1996; Guddat, Bardwell, Glockshuber *et al.*, 1997; Hennecke *et al.*, 1997; Jacobi *et al.*, 1997; Huber-Wunderlich & Glockshuber, 1998; Warwicker, 1998). In cpDsbA$_{Q100T99}$ all these residues have acquired new conformations and a new local environment. However, no significant change in the redox potential and catalytic activity is observed for cpDsbA$_{Q100T99}$ (Hennecke *et al.*, 1999). The redox potential of cpDsbA$_{Q100T99}$ is only 5 mV more oxidizing than DsbA and the enzyme even proved to be slightly more efficient as a stoichiometric oxidant and disulfide isomerase during refolding of the thrombin inhibitor hirudin *in vitro* (Hennecke *et al.*, 1999). From the only slightly reduced redox potential of cpDsbA$_{Q100T99}$, we can also predict that the pK_a of Cys30 is still extremely low and has a value of $\sim$3.7 (Mossner *et al.*, 2002). This indicates that cpDsbA$_{Q100T99}$ has retained both the reactivity of the catalytic disulfide bond towards polypeptide substrates and the ability to interact with substrates. In addition, the fact that the conformations of many residues in the substrate-binding region of DsbA are altered in cpDsbA$_{Q100T99}$ is in line with the observation that DsbA is poorly optimized for substrate peptide binding, which is 10^4-fold tighter in the periplasmic disulfide isomerase DsbC (Guddat, Bardwell, Zander *et al.*, 1997). The switching of

hydrogen bonding between Gln97, Cys30 and Phe29 and the changed interaction network of the charged residues Glu24, Glu37 and Glu58 may also contribute to the retained oxidative power of cpDsbA$_{Q100T99}$.

Oxidized cpDsbA$_{Q100T99}$ is slightly less stable than oxidized wild-type DsbA, -44.1 kJ mol^{-1} for cpDsbA$_{Q100T99}$ compared with -48.7 kJ mol^{-1} for the wild type (Hennecke *et al.*, 1999). A possible explanation could be that its multiple local conformational changes relative to DsbA are partially compensated for by reduced electrostatic repulsion of Glu94 and Glu38 and an increased entropy of the native state owing to retained flexibility around the natural termini and additional flexibility around the new termini.

Financial support by the Alexander von Humboldt Foundation through a research fellowship to AMB and by the Fonds der Chemischen Industrie is gratefully acknowledged.

References

Aÿ, J., Hahn, M., Decanniere, K., Piotukh, K., Borriss, R. & Heinemann, U. (1998). *Proteins Struct. Funct. Genet.* **30**, 155–167.

Bardwell, J. C., McGovern, K. & Beckwith, J. (1991). *Cell*, **67**, 581–589.

Barrientos, L. G., Louis, J. M., Ratner, D. M., Seeberger, P. H. & Gronenborn, A. M. (2003). *J. Mol. Biol.* **325**, 211–223.

Cheltsov, A. V., Guida, W. C. & Ferreira, G. C. (2003). *J. Biol. Chem.* **278**, 27945–27955.

Chu, V., Freitag, S., Le Trong, I., Stenkamp, R. E. & Stayton, P. S. (1998). *Protein Sci.* **7**, 848–859.

Collet, J. F. & Bardwell, J. C. (2002). *Mol. Microbiol.* **44**, 1–8.

Esnouf, R. M. (1999). *Acta Cryst.* D**55**, 938–940.

Gane, P. J., Freedman, R. B. & Warwicker, J. (1995). *J. Mol. Biol.* **249**, 376–387.

Goldenberg, D. P. & Creighton, T. E. (1983). *J. Mol. Biol.* **165**, 407–413.

Graf, R. & Schachman, H. K. (1996). *Proc. Natl Acad. Sci. USA*, **93**, 11591–11596.

Guddat, L. W., Bardwell, J. C., Glockshuber, R., Huber-Wunderlich, M., Zander, T. & Martin, J. L. (1997). *Protein Sci.* **6**, 1893–1900.

Guddat, L. W., Bardwell, J. C. & Martin, J. L. (1998). *Structure*, **6**, 757–767.

Guddat, L. W., Bardwell, J. C., Zander, T. & Martin, J. L. (1997). *Protein Sci.* **6**, 1148–1156.

Hahn, M., Piotukh, K., Borriss, R. & Heinemann, U. (1994). *Proc. Natl Acad. Sci. USA*, **91**, 10417–10421.

Heinemann, U. & Hahn, M. (1995*a*). *Prog. Biophys. Mol. Biol.* **64**, 121–143.

Heinemann, U. & Hahn, M. (1995*b*). *Trends Biochem. Sci.* **20**, 349–350.

Hennecke, J., Sebbel, P. & Glockshuber, R. (1999). *J. Mol. Biol.* **286**, 1197–1215.

Hennecke, J., Spleiss, C. & Glockshuber, R. (1997). *J. Biol. Chem.* **272**, 189–195.

Hu, S. H., Peek, J. A., Rattigan, E., Taylor, R. K. & Martin, J. L. (1997). *J. Mol. Biol.* **268**, 137–146.

Huber-Wunderlich, M. & Glockshuber, R. (1998). *Fold. Des.* **3**, 161–171.

Iwakura, M., Nakamura, T., Yamane, C. & Maki, K. (2000). *Nature Struct. Biol.* **7**, 580–585.

Jacobi, A., Huber-Wunderlich, M., Hennecke, J. & Glockshuber, R. (1997). *J. Biol. Chem.* **272**, 21692–21699.

Jones, T. A., Zou, J. Y., Cowan, S. W. & Kjeldgaard, M. (1991). *Acta Cryst.* A**47**, 110–119.

Jung, J. & Lee, B. (2001). *Protein Sci.* **10**, 1881–1886.

Kortemme, T., Darby, N. J. & Creighton, T. E. (1996). *Biochemistry*, **35**, 14503–14511.

Kraulis, P. J. (1991). *J. Appl. Cryst.* **24**, 946–950.

Li, L. & Shakhnovich, E. I. (2001). *J. Mol. Biol.* **306**, 121–132.

Lindqvist, Y. & Schneider, G. (1997). *Curr. Opin. Struct. Biol.* **7**, 422–427.

Luger, K., Hommel, U., Herold, M., Hofsteenge, J. & Kirschner, K. (1989). *Science*, **243**, 206–210.

Martin, J. L., Bardwell, J. C. & Kuriyan, J. (1993). *Nature (London)*, **365**, 464–468.

Merritt, E. A. & Murphy, M. E. P. (1994). *Acta Cryst.* D**50**, 869–873.

Mossner, E., Iwai, H. & Glockshuber, R. (2002). *FEBS Lett.* **477**, 21–26.

Murshudov, G. N., Vagin, A. A. & Dodson, E. J. (1997). *Acta Cryst.* D**53**, 240–255.

Murzin, A. G. (1998*a*). *Curr. Opin. Struct. Biol.* **8**, 380–387.

Murzin, A. G. (1998*b*). *Nature Struct. Biol.* **5**, 101.

Navaza, J. (2001). *Acta Cryst.* D**57**, 1367–1372.

Nelson, J. W. & Creighton, T. E. (1994). *Biochemistry*, **33**, 5974–5983.

Otwinowski, Z. & Minor, W. (1997). *Methods Enzymol.* **276**, 307–326.

Perrakis, A., Harkiolaki, M., Wilson, K. S. & Lamzin, V. S. (2001). *Acta Cryst.* D**57**, 1445–1450.

Pieper, U., Hayakawa, K., Li, Z. & Herzberg, O. (1997). *Biochemistry*, **36**, 8767–8774.

Potterton, E., Briggs, P., Turkenburg, M. & Dodson, E. (2003). *Acta Cryst.* D**59**, 1131–1137.

Ritz, D. & Beckwith, J. (2001). *Annu. Rev. Microbiol.* **55**, 21–48.

Rojas, A., Santiago, G.-V., Jaume, P. & Antoni, R. (1999). *Biologia (Bratislava)*, **54**, 255–277.

Schirra, H. J., Renner, C., Czisch, M., Huber-Wunderlich, M., Holak, T. A. & Glockshuber, R. (1998). *Biochemistry*, **37**, 6263–6276.

Thornton, J. M. & Sibanda, B. L. (1983). *J. Mol. Biol.* **167**, 443–460.

Tougard, P., Bizebard, T., Ritco-Vonsovici, M., Minard, P. & Desmadril, M. (2002). *Acta Cryst.* D**58**, 2018–2023.

Uliel, S., Fliess, A. & Unger, R. (2001). *Protein Eng.* **14**, 533–542.

Viguera, A. R., Serrano, L. & Wilmanns, M. (1996). *Nature Struct. Biol.* **3**, 874–880.

Warwicker, J. (1998). *J. Biol. Chem.* **273**, 2501–2504.

Winn, M. D., Isupov, M. N. & Murshudov, G. N. (2001). *Acta Cryst.* D**57**, 122–133.

Wright, G., Basak, A. K., Wieligmann, K., Mayr, E. M. & Slingsby, C. (1998). *Protein Sci.* **7**, 1280–1285.

Wunderlich, M., Jaenicke, R. & Glockshuber, R. (1993). *J. Mol. Biol.* **233**, 559–566.

Wunderlich, M., Otto, A., Maskos, K., Mucke, M., Seckler, R. & Glockshuber, R. (1995). *J. Mol. Biol.* **247**, 28–33.

Zapun, A., Bardwell, J. C. & Creighton, T. E. (1993). *Biochemistry*, **32**, 5083–5092.

Zapun, A., Cooper, L. & Creighton, T. E. (1994). *Biochemistry*, **33**, 1907–1914.